Synthesis of ultrafine titania nano-cages by pulsed laser ablation of Ti/Al alloy in ammonium hydroxide

Dameng Wang (王大猛)[1], Ming Chen (陈 明)[1], Xiangdong Liu (刘向东)[1,*], and Xueping Gao (高学平)[2,]**

[1]*School of Physics and State Key Laboratory of Crystal Materials, Shandong University, Jinan 250100, China*
[2]*School of Materials Science and Engineering, Shandong University, Jinan 250061, China*
**Corresponding author: xdliu@sdu.edu.cn; **corresponding author: xpgao@sdu.edu.cn*
Received April 13, 2015; accepted June 19, 2015; posted online July 7, 2015

A simple and versatile strategy is designed to successfully fabricate ultrafine TiO_2 nano-cages based on the rapid decomposition reaction between amphoteric hydroxide and ammonia solution by pulsed laser ablation of Ti/Al alloy in liquid. With the ammonia concentration ($V_{ammonia}$:V_{water}, where V is volume) increasing from 1:10 to 1:4, the diameter and shell thickness of quasi-spherical TiO_2 nano-cages substantially decrease from 300 and 60 nm to 9.2 and 2.8 nm, respectively. The obtained results have significant implications for obtaining insight into the properties of the TiO_2 porous nano-cages, offering the basis for further fabrication of other nano-cages.

OCIS codes: 140.3440, 350.3850.
doi: 10.3788/COL201513.081404.

Nano-sized TiO_2 inorganic semiconductors as wide band gap semiconductors exhibit a wide range of electrical and optical properties, which are strongly affected by their structures, heterogeneous interfaces, and exposed faces. Hollow-like TiO_2 nano-cages are characterized as fine structures with lower densities, higher permeability, and larger specific surface area, which have attracted considerable research attention in recent years owing to their extensive use in photo-catalysts, dye-sensitized solar cells (DSSC), and fast responsive sensors[1,2]. Additionally, TiO_2 nano-cages are thought to be the most suitable material for removing organic pollutants in wastewater due to their biocompatibility, photostability, chemical inertness, and favorable band position[3–6]. Increasing evidence has proven that the properties of TiO_2 nano-cages are highly related to their hollow interiors and porous shells[1,7]. Therefore, a simple, versatile, and rapid route to controllably synthesize TiO_2 nano-cages with a designed shape and geometry is of great significance for specific applications.

In the design of hollow nano-materials, the available synthesis methods, such as the template-based method[1], thermal evaporation[6], and solvothermal[8], laser ablation of a solid or dispersed target in liquid solutions (LAL), without use of chemical catalysts or additives, represents an attractive technique with its highly nonequilibrium processing character. Moreover, colloidal nano-particles synthesized by laser fabrication in liquid exhibit novel metastable phases by the addition of ionic surfactants[8–12]. Many interesting results such as fabrication of hollow MgO nano-structures[12], Al_2O_3 nano-cages[13], and ZnO porous structures[8] have been reported using laser ablation in liquid. Compared with these reactive objects, it should be noted that some other nano-materials, such as SiO_2, TiO_2 possesses solid interiors[14–17], and the nano-cages a hard to produce directly from the bulk target by generated bubbles via bubble surface pinning during laser ablation.

Recently, we reported an experiment[10] in which ZnO nano-cages with hollow spaces were fabricated by using laser ablation of a Zn target in ammonium hydroxide, owing to the decomposition reaction that occurred between amphoteric hydroxide and ammonia liquid. As known, the evidence confirmed that laser ablation of a Ti target in distilled water will result in TiO_2 nano-particles with solid interiors, as opposed to nano-cages that form in liquid[16]. In this work, we developed a simple and versatile route using a Ti/Al alloy as the target and ammonia liquid as the laser ablation condition, to the large-scale synthesis of TiO_2 nano-cages with well-defined hollow interiors. The key step of this process involves a similar decomposition reaction between amphoteric hydroxide and ammonia during laser ablation of Ti/Al alloy in weak alkaline conditions. The aim of this work is to extend the scope of porous nano-cages that laser ablation in liquid can fabricate. The relevant mechanism obtained from the theoretical models and experiments reported in this Letter have significant implications for obtaining insight into the properties of TiO_2 nano-cages, offering the basis for further development of reliable applications.

The present experimental scheme used for generation of TiO_2 nano-cages is similar to that used in previous studies[5,8–12]. In summary, a well-polished Ti/Al (1:1) alloy is used as a target placed on the bottom of a rotating glass dish filled to a 3-mm depth with a liquid medium containing deionized water and ammonia ($V_{ammonia}$:V_{water} = 1:10 to 1:4, where V = volume). A 1064 nm laser beam with a pulse duration of 10 ns and 5 Hz repetition rate from a YAG laser (Quanta Ray, Spectra Physics) was focused on the target by a quartz lens with a 40 mm focal

length. The incident power density was approximately 4 GW/cm^2 for all tests, and the ablation lasted for 30 min. We found that the power density played a critical role for the ablation product, below or above which only some clusters or bulk molten droplets were formed in the liquid. After the laser ablation, precipitates of the products were repeatedly centrifuged at 2503 g for 20 min by an ultracentrifuge, and the obtained materials were washed with ethanol 4 times to remove ammonia. The sediments were dropped on a copper mesh covered with an amorphous carbon film and dried in an oven at 45°C in air for observation by transmission electron microscopy (TEM; JEOL-JEM-2100F). A field emission scanning electron microscope (Hitachi S-4800) equipped for energy-dispersive X-ray spectroscopy (EDS) was employed to indentify the morphological structures and chemical compositions.

As for the pulsed laser ablation of Ti/Al alloy in liquid, it is necessary to reveal the formation of TiO_2/$Al(OH)_3$ hybrid nano-composites, which should be considered as a precursor for the generation of final TiO_2 nano-cages in ammonia conditions. After laser ablation of the Ti/Al alloy target in deionized water, the typical low-magnification [Fig. 1(a)] and enlarged [Fig. 1(b)] morphologies of the hybrid nano-particles were analyzed by TEM. The overall TEM image in Fig. 1(a) clearly shows numerous spherical nano-materials with diameters varying from 260 to 320 nm. One point to emphasize is that the homogeneous distributions of these spherical nano-materials imply that they are likely individually fabricated, one-by-one, since there are almost no hinge joints. Close inspection of the representative nano-material in Fig. 1(b) illustrates that the morphology of the well-defined specimen is characterized by a highly center-symmetrical spherical-shaped structure, exhibiting a rather smooth surface. The spherical-shaped materials are amorphous nanostructures as shown in the selected area electron diffraction (SAED) image [Fig. 1(c)]. The energy dispersive X-ray (EDX) spectrum and EDS mappings of the distribution of a single spherical-shaped structure are shown in Fig. 1(d), demonstrating the existence of Ti, Al, and O elements. The elemental Ti and Al signals were found throughout the particles, from the inner core to the periphery. In principle, some light elements, such as hydrogen, can be detected in neither EDX nor EDS patterns. The question of the compositions of these compounds will be reasonably solved in the follow discussion.

First, Ti and Al ions should be produced in the plasma by nanosecond pulsed-laser ablation of the Ti/Al target in ammonia solution. Based on previous work[5], titanium hydroxide is an extremely unstable compound material; it is rapidly decomposed to TiO_2 and H_2O at normal temperature. In contrast, $Al(OH)_3$ remains stable at ~300°C. In addition, the result of the EDS in Fig. 1(d) clearly demonstrates that the ratio of Ti, Al, to O in the nano-spheres is about 12:16:71, which can be approximated to 1:1:5. It is reasonable to deduce that the spherical-shaped amorphous material by laser ablation of Ti/Al in water should be TiO_2/$Al(OH)_3$ hybrid nano-composites with a ratio of about 1:1.

The $Al(OH)_3$ byproduct is amphoteric hydroxide, which will dissolve in weakly alkaline conditions by the decomposition reaction. The scanning electron microscopy (SEM) image and EDS results of the TiO_2/$Al(OH)_3$ hybrid nano-composites are shown in Figs. 2(a) and 2(c), respectively. By the addition of ammonia to the colloidal solution, the hybrid nano-composites indeed have different morphologies, as per the SEM image and EDS pattern shown in Figs. 2(b) and 2(d). Compared with the center-symmetrical nano-spheres with smooth surfaces in Fig. 2(a), the different morphology in Fig. 2(b) presents that the representative nano-sphere is characterized by the absolute

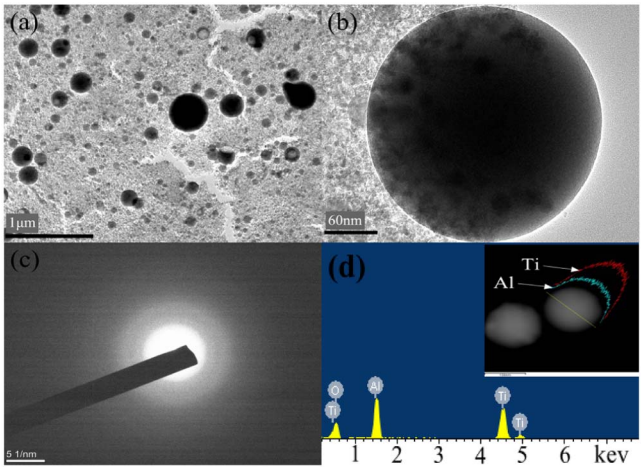

Fig. 1. (a) Overall and (b) representative TEM images of hybrid nano-particles synthesized by pulsed laser ablation of a Ti/Al alloy in deionized water; (c) corresponding SAED pattern; (d) EDX spectrum and EDS mappings of the constitute distribution of a spherical-shaped structure.

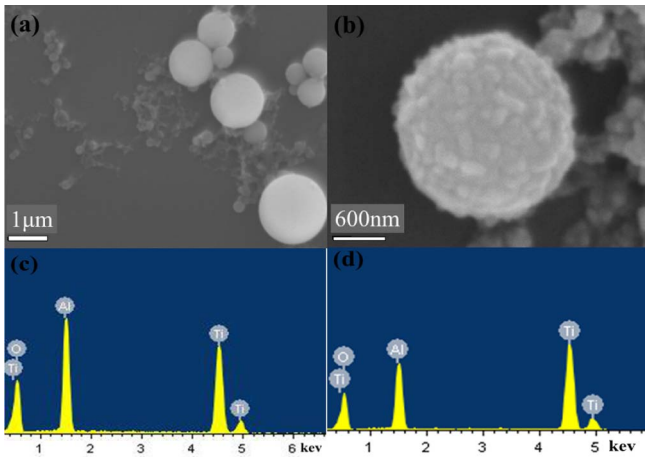

Fig. 2. (a) SEM images of TiO_2/$Al(OH)_3$ hybrid nano-composites generated in deionized water; (b) typical SEM images of a hybrid nano-particle obtained by the addition of ammonia to the colloidal solution; (c) EDS pattern of TiO_2/$Al(OH)_3$ hybrid nano-composites generated in deionized water; (d) corresponding EDS pattern.

roughness surface. The rough surface of the hybrid nano-composites implies that some $Al(OH)_3$ byproducts can be dissolved and removed from the $TiO_2/Al(OH)_3$ hybrid nano-composites, because a reaction occurs between the hydroxide and activated liquid. In addition, this mechanism can be clearly confirmed by the ratio of the chemical composition. The EDS results in Fig. 2(c) demonstrates that the ratio of Ti, Al, and O is about 12:15:72, whereas the EDS pattern in Fig. 2(d) is about 21:19:70. The relative proportion of the Al chemical composition decreases after the addition of ammonia to the $TiO_2/Al(OH)_3$ hybrid nano-composites. If the ablation of Ti/Al alloy is carried out in a liquid phase containing ammonia hydroxide, the ablated $Al(OH)_3$ material can be dissolved and removed from the $TiO_2/Al(OH)_3$ hybrid nano-composites. Then TiO_2 nano-cages will be obtained due to the decomposition reaction that occurs between the aluminum hydroxide and the activated liquid.

Finally, well-defined TiO_2 nano-cages were fabricated by pulsed laser ablation of Ti/Al alloy in liquid medium containing deionized water and ammonia ($V_{ammonia}$: V_{water} = 1:10 to 1:4). As per cumulative pulse laser ablation in liquid solution ($V_{ammonia}$:V_{water} = 1:10), typical TEM images of TiO_2 nano-cages are shown in Fig. 3(a). The morphology of the product in Fig. 3(a) clearly shows that the quasi-spherical TiO_2 particle is indeed a nano-cage structure with an interior cavity. According to the statistics, the average diameter of the final TiO_2 nano-cages is approximately 300 nm, and shell thickness of the cages is about 60 nm. It should be noted that the lower concentration of ammonia in the liquid provides some incomplete or multilayer cavity structure in TiO_2 nano-cages. Moreover, close inspection of the TiO_2 nano-cages demonstrates that numerous nano-scaled clusters with fabric-like structures were accreted on the surfaces of the hollow structures. The material inside the nano-cages should be $TiO_2/Al(OH)_3$ hybrid clusters, which have been examined by using TEM image analysis. The multilayer cavity and numerous clusters should be explained by the incomplete decomposition of the aluminum hydroxide material during laser ablation of Ti/Al alloy in low ammonia concentrations. Following this mechanism, a higher concentration of ammonia liquid should result in a larger space in the TiO_2 nano-cages. To verify this mechanism, we increased the concentration of ammonia via deionzed liquid to 1:7, and found that the typical TiO_2 nano-cage exhibits an incomplete or multilayer cavity structure and slightly smooth surface [Fig. 3(b)]. The average diameter of the products is about 160 nm, which is much smaller than that in Fig. 3(a). The porous shell thickness of a TiO_2 nano-cage is measured as about 60 nm, which is similar to that obtained in lower ammonia concentrations. As for the ammonia concentration increasing to 1:4, in comparison with the morphologies displayed in Figs. 3(a) and 3(b), the TiO_2 nano-cage significantly changes [Fig. 3(c)]. An individual TiO_2 nano-cage is characterized by an obvious interior cavity and clearly smooth shell. The nano-cage size and the shell thickness are about 35 and

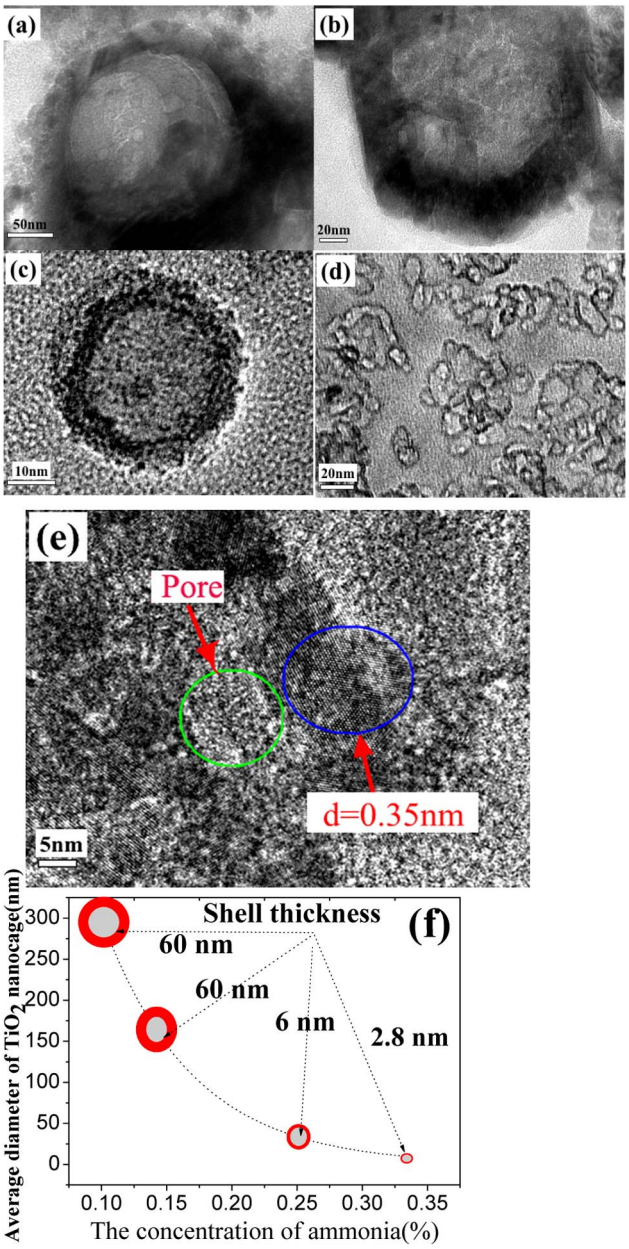

Fig. 3. Typical TEM images of TiO_2 nano-cages fabricated by laser ablation of Ti/Al alloy in liquid, where $V_{ammonia}$:V_{water} is the following: (a) 1:10; (b) 1:7; (c) 1:4; (d) 1:3; (e) HRTEM image of representative TiO_2 nano-cages obtained at an ammonia concentration of 1:3; (f) diameters and the shell thicknesses of spherical TiO_2 nano-cages versus the ammonia concentration.

6 nm, respectively, which are noticeably smaller than the measured in Figs. 3(a) and 3(b). Further increasing the ammonia concentration to 1:3, well-defined ultrafine TiO_2 nano-cages were obtained [Fig. 3(d)]. The more fascinating structures observed in Fig. 3(d) show that ultrafine nano-cages with a clearly hollow interior space and a distinctive porous shell tend to interconnect with each other via a magnetic–dipole interaction, and then form short curvilinear groups with necklace-like structures. According to the statistics, the average diameter of the

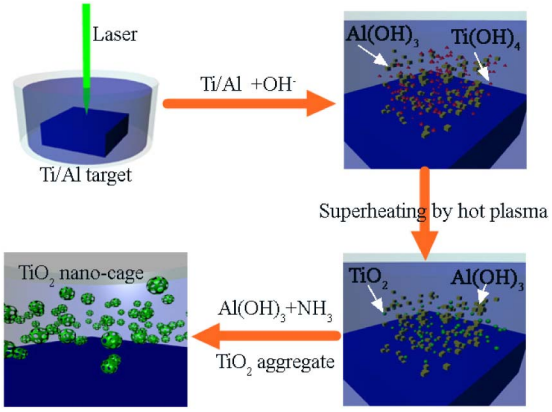

Fig. 4. Schematic of the growth diagram of TiO_2 porous nano-cages by laser ablation of a Ti/Al alloy in aqueous ammonia.

final TiO_2 nano-cages is about 9.2 nm, and the shell thickness is about 2.8 nm. Moreover, the high-re solution transmission electron microscopy (HRTEM) image in Fig. 3(e) illustrates that the porous nano-cages structure is found to be well-crystalline according to the clear fringes, yet obvious surface pores with a size of 2–4 nm. The pores in the nano-cages are shown as contrasting lighter images with their walls as darker images, due to different penetration depths of the incident electron beam. Correspondingly, the lattice fringe with a spacing of 0.35 nm can be identified for the TiO_2 (101) plane. Moreover, the diameters and the shell thicknesses of spherical-like TiO_2 nano-cages versus the ammonia concentration are briefly summarized [Fig. 3(f)]. The curves of nano-cage dimension versus alkaline concentrations can be described as an exponential function.

In the following, we describe the possible processes for the formation of TiO_2 nano-cages, which has been verified in our previous work[10]. The ablation of Ti/Al alloy is carried out in a liquid phase containing some ammonia hydroxide; the possible growth process for the formation of TiO_2 porous nano-cages is described as per the schematic diagram shown in Fig. 4. In brief, the growth mechanism of the final structure involves the generation of $Ti(OH)_4$ and $Al(OH)_3$ materials first. In the laser ablation (0–10 ns) process, superheating will play a critical role in the early stage. Most $Ti(OH)_4$ materials are rapidly decomposed into TiO_2 by the hot plasma and immediately mixed with the remainder of the $Al(OH)_3$ material, which them results in the initial formation of $TiO_2/Al(OH)_3$ hybrid composites. Meanwhile, the extreme conditions characterized by the highly nonequilibrium feature including high temperature and high pressure[10–17] will result in an ultra-rapid alkaline etching process within a single laser pulse (10 ns). The temperature around the ablated crater is much higher, which enhances the chemical reaction. The ultra-rapid chemical reaction enables the $Al(OH)_3$ to be dissolved/removed from $TiO_2/Al(OH)_3$ hybrid composites. Then TiO_2 nano-cages will be obtained due to the decomposition reaction occurring between aluminium hydroxide and the activated liquid. The higher ammonia concentration results in a more complete decomposition reaction. The ultra-rapid reaction in a confined space enables the formation of abundant voids in the final particles. Overall, based on the experimental results reported in this Letter, we demonstrate that the ammonia concentration plays a critical role in the final nano-cages, and the liquid solution is readily adjusted to obtain desirable TiO_2 nano-cages.

In conclusion, TiO_2 porous nano-cages are synthesized through pulsed laser ablation of a Ti/Al alloy in ammonia solution. The weakly alkaline solution plays an import role in the fabrication of desirable nano-cages. A higher concentration of ammonia can improve the degree of decomposition of the aluminum hydroxide material due to the ultra-rapid alkaline etching in hotter plasma during the laser ablation process. Then, ultrafine TiO_2 nano-cages with a controllable interior space and a distinctive porous shell should be obtained with higher ammonia concentrations. The synthetic scheme used here should also be applicable to other metals.

This work was supported by the National Natural Science Foundation of China (Nos. 11105085, 11275116, and 11375108), the Excellent Youth and Middle Age Scientists Fund of Shandong Province (No. BS 2012CL024), and the Fundamental Research Funds of Shandong University (No. 2015JC007).

References

1. M. C. Tsai, M. H. Yang, Y. W. Chang, J. K. Tzeng, C. Y. Lee, H. T. Chiu, H. C. Chen, and I. N. Lin, Mater. Chem. Phys. **143**, 60 (2013).
2. J. G. Yu, Y. R. Su, and B. Cheng, Adv. Funct. Mater. **17**, 1984 (2007).
3. Y. Gu, C. Cai, Q. Feng, and Y. Li, Chin. Opt. Lett. **12**, 091602 (2014).
4. T. Harada, H. Murotani, S. Matumoto, and H. Honda, Chin. Opt. Lett. **11**, S10303 (2013).
5. A. Nath, S. S. Laha, and A. Khare, Appl. Surf. Sci. **257**, 3118 (2011).
6. A. Umar and Y. B. Hahn, Appl. Surf. Sci. **254**, 3339 (2008).
7. Y. Xue, J. Lin, Y. Fan, A. Elsanousi, X. Xu, J. Mi, J. Li, X. Zhang, Y. Lu, T. Zhang, and C. Tang, Mater. Chem. Phys. **143**, 446 (2013).
8. A. Pan, R. Yu, S. Xie, Z. Zhang, C. Jin, and B. Zou, J. Cryst. Growth **282**, 165 (2005).
9. A. Thankappan, S. Thomas, and V. P. N. Nampoori, Chin. Opt. Lett. **11**, 101801 (2013).
10. S. Li, M. Chen, and X. D. Liu, Opt. Express **22**, 18707 (2014).
11. Z. J. Yan, R. Q. Bao, and D. B. Chrisey, Chem. Phys. Lett. **497**, 205 (2010).
12. Z. J. Yan, R. Q. Bao, C. M. Busta, and D. B. Chrisey, Nanotechnology **22**, 265610 (2011).
13. Z. J. Yan, R. Q. Bao, Y. Huang, and D. B. Chrisey, J. Phys. Chem. C **114**, 11370 (2010).
14. J. Yang, F. F. Luo, T. S. Kao, X. Li, G. Ho, J. H. Teng, X. G. Luo, and M. H. Hong, Light Sci. Appl. **3**, e185 (2014).
15. J. Yang, J. B. Li, Q. H. Gong, J. H. Teng, and M. H. Hong, Nanotechnology **25**, 465707 (2014).
16. C. H. Liu, M. H. Hong, Y. Zhou, G. X. Chen, M. M. Saw, and A. T. S. Hor, Phys. Scr. **T129**, 326 (2007).
17. F. F. Luo, Y. C. Guan, W. Ong, Z. R. Du, G. Ho, F. P. Li, S. F. Sun, G. Lim, and M. H. Hong, Opt. Express. **22**, 23875 (2014).